Adaptive Spatial Resolution in Fast, Efficient, and Stable Analysis of Metallic Lamellar Gratings at Microwave Frequencies

Amin Khavasi and Khashayar Mehrany

***Abstract*—the technique of adaptive spatial resolution is for the first time applied in fast and efficient Fourier-based analysis of metallic lamellar gratings at microwave frequencies. Inasmuch as the ultrahigh-contrast permittivity profile of these structures is likely to incur numerical instabilities, the continuity condition is heedfully imposed on the transverse electromagnetic fields and an elegant, unconditionally stable matrix-based strategy is proposed to rigorously analyze the microwave transmission of these structures.**

***Index Terms*—metallic grating, adaptive spatial resolution, enhanced transmission.**

I. Introduction

DIFFRACTION analysis of metallic gratings at microwave and radio frequencies is an extensively well-studied topic, which; thanks to the duet features of frequency and polarization selectivity, has received plentiful attention in the past half-century [1]-[8]. The recently discovered enhanced transmission of optical waves through two-dimensional metallic arrays of subwavelength holes [9], however, was a brand new phenomenon that revived the general interest in the electromagnetic diffraction by metallic gratings with sub-wavelength features, and, accordingly, granted a new lease on life to numerical and experimental study of microwave transmission through metallic gratings [10]-[16]. Yet, most of the reported numerical studies at microwave frequencies depend on the brute force and time consuming numerical techniques in the real space, e.g. the finite difference time domain (FDTD) [13], and the finite element method (FEM) [15]. This is in contrast to the availability of dozens of semi-analytical fast and efficient simulation methods in optical regime. Aside minor technical differences, all these methods are based on the Fourier expansion of the periodic permittivity profile [17]-[19], and are capable of efficiently analyzing metallic gratings in the so called reciprocal space [20]. The inaccessibility of the fast and efficient Fourier based methods in the microwave regime is to a certain extent inevitable since the imaginary part of the permittivity, i.e. normalized conductivity, of metals at these frequencies becomes awfully large, and contrasts sharply with the permittivity of the neighboring dielectric; usually air, slits. This sharp contrast turns to be terribly troublesome as the Fourier expansion of the discontinuous permittivity profile of the structure should be unavoidably truncated in computer calculations, and consequently suffers from the Gibbs phenomenon, has an extremely low convergence speed, and is gravely erroneous unless a large number of Fourier components are retained.

This problem is here tackled by applying the technique of adaptive spatial resolution (ASR), which employs a new coordinate system to increase the spatial resolution around the discontinuities of the permittivity profile [21]. This mathematical stratagem can substantially improve the overall rate of convergence and has already proved useful in analyzing lamellar and trapezoidal gratings at optical frequencies [21]-[23]. It has been more recently reformulated in an easy-to-program matrix form, which evades the eigenvalue problem in the neighboring homogeneous regions and can be easily applied to multilevel profiles [23]. These two latter advantages are however bought at the expense of conditional stability, which, by the way, is a very important issue at microwave frequencies, where a large number of space harmonics, i.e. Fourier components, are to be retained. This problem is here fixed by duly rearranging the matrix equations, thanks to which the unconditional stability is guaranteed. In this fashion, electromagnetic diffraction of highly conducting lamellar gratings in general and the enhanced microwave transmission in particular can be very efficiently studied. It should be however noticed that the proposed method is limited to single section structures and is currently presented for highly conducting single section lamellar gratings.

This paper is organized as follows: the mathematical foundation of the ASR technique is briefly reviewed in section II. An unconditionally stable implementation of the boundary conditions by using the S-matrix propagation algorithm in the transformed coordinate system is presented in section III, and the reflection and transmission coefficients are then found in a simple and stable way. Various numerical examples are provided in section IV, whereby the applicability and efficiency of the proposed method are attested. Finally, conclusions are made in section V.

Manuscript received June 08, 2008.

The authors are with Electrical Engineering Department, Sharif University of Technology, Tehran, Iran (e-mail: mehrany@ sharif.edu).

II. MATHEMATICAL FOUNDATION

Consider a typical lamellar grating configuration as shown in Fig. 1. The metallic grating region with thickness d is characterized by a piecewise constant periodic permittivity profile $\varepsilon(x)=\varepsilon(x+\Lambda_g)$ which separates two homogeneous media with refractive indices n_1 and n_3. In accordance with Fig. 1, the permittivity profile $\varepsilon(x)$ on each interval of constancy between neighboring jump points; i.e. for $x_{l-1} < x < x_l$, is equal to either ε_d (dielectric), or ε_m (metal). The complex permittivity of the metal ε_m in the SI system; however, can be written in terms of the metal conductivity σ, and the free space wavelength λ_0 [1]:

$$\varepsilon_m = 1 - j60\sigma\lambda_0 \tag{1}$$

This structure is illuminated by a linearly polarized monochromatic uniform plane wave whose wave vector in region 1 is inclined at the angle θ to the Oz axis.

The transverse electromagnetic fields can then be easily found by applying the rigorous coupled wave analysis (RCWA), also called the Fourier modal method (FMM), whereby the original wave equation takes the form of a standard eigenvalue problem in the discrete Fourier space [17]

$$\lambda_q^2 \mathbf{E}_y = \left[\mathbf{K}_x^2 - k_0^2 [\![\varepsilon]\!]\right]\mathbf{E}_y \tag{2}$$

for TE polarization, and

$$\lambda_q^2 \mathbf{H}_y = \left[[\![1/\varepsilon]\!]^{-1}\left(\mathbf{K}_x [\![\varepsilon]\!]^{-1}\mathbf{K}_x - k_0^2\right)\right]\mathbf{H}_y \tag{3}$$

for TM polarization. Here, k_0 is the vacuum wavenumber, $[[f]]$ denotes the Toeplitz matrix whose (m, n) entry is the $(m–n)$th Fourier coefficient of $f(x)$; hereafter denoted by f_{m-n}, and $\mathbf{K}_x$ stands for the diagonal matrix whose ith diagonal element is,

$$k_{xi} = k_0 n_1 \sin\theta - \frac{2\pi}{\Lambda_G} i \tag{4}$$

The eigenvalues λ_q^2s and their corresponding eigenvectors $\mathbf{E}_y$ for the TE polarization and $\mathbf{H}_y$ for the TM polarization then make up the electromagnetic field distribution.

Despite being among the simplest and the most efficient semi-analytical methods available at the optical frequencies [17], this approach cannot be efficiently exercised in the microwave range because the equivalent complex permittivity ε_m of the metallic region is much larger than the dielectric permittivity ε_d, the convergence rate of the Fourier series of the piecewise-constant permittivity profile $\varepsilon(x)$ is awfully slow, and consequently the sizes of the matrices involved in equations (2) and (3) are quite imposing. This problem can, however, be considerably ameliorated if the Cartesian coordinate x is appropriately replaced by a new coordinate u, which transforms the wave equation into the following eigenvalue problem in a new discrete Fourier space [23]

$$\lambda_q^2 \mathbf{E}_y = \left[-[\![h]\!]^{-1}\left(k_0^2 [\![\varepsilon h]\!] - \mathbf{K}_x [\![h]\!]^{-1}\mathbf{K}_x\right)\right]\mathbf{E}_y \tag{5}$$

for TE polarization, and

$$\lambda_q^2 \mathbf{H}_y = \left[-[\![h/\varepsilon]\!]^{-1}\left(k_0^2 [\![h]\!] - \mathbf{K}_x [\![\varepsilon h]\!]^{-1}\mathbf{K}_x\right)\right]\mathbf{H}_y \tag{6}$$

for TM polarization. Here, $h(u)$ denotes the resolution function, and is determined by the dependence between x and u coordinates [23]:

$$h(u) = \frac{dx}{du} \tag{7}$$

It can be easily seen that the Toeplitz matrices formed from the Fourier series of the ultrahigh-contrast functions $\varepsilon(x)$ and $\varepsilon^{-1}(x)$ in the original equations (2-3) are now replaced by the Toeplitz matrices corresponding to the new functions $h(u)\varepsilon(u)$ and $h(u)\,\varepsilon^{-1}(u)$ in the transformed equations (5-6). These functions should be smooth enough to guarantee the fast convergence of their corresponding Fourier series. Now, if the resolution function $h(u)$ is almost zero at $u=u_l$ corresponding to the former jump points $x=x_l$ in the Cartesian coordinate system shown in Fig. 1, then the abovementioned functions $h(u)\varepsilon(u)$ and $h(u)\,\varepsilon^{-1}(u)$ are much smoother, can be accurately approximated by keeping not a very large number of Fourier terms, and result in Toeplitz matrices of manageable size. In this manuscript, the coordinate u is chosen in accordance with what is proposed by Vallius *et al.* [23]:

$$x(u) = a_1 + a_2 u + \frac{a_3}{2\pi}\sin\left(2\pi\frac{u-u_{l-1}}{u_l - u_{l-1}}\right) \tag{8-a}$$

where,

$$a_1 = \frac{u_l x_{l-1} - u_{l-1} x_l}{u_l - u_{l-1}} \tag{8-b}$$

$$a_2 = \frac{x_l - x_{l-1}}{u_l - u_{l-1}} \tag{8-c}$$

$$a_3 = G\left(u_l - u_{l-1}\right) - \left(x_l - x_{l-1}\right) \tag{8-d}$$

and G is an almost zero constant, here chosen to be G = 0.001.

This transformation meets the abovementioned criterion of being almost zero at $u=u_l$, and shows a good convergence even in the microwave range, where the original permittivity function is very hard to be approximated by its truncated Fourier series.

Having chosen a fitting coordinate u, like the one given in equations (8), the electromagnetic field distribution can be expressed in terms of the eigenvalues and eigenvectors of

equations (5-6)

$$\Psi^{(p)} = \sum_{q=-N}^{N} [A_q^{(p)} \exp\left(\lambda_q^{(p)} z\right) + B_q^{(p)} \exp\left(-\lambda_q^{(p)} z\right) \cdot \sum_{m=-N}^{N} \Psi_{mq}^{(p)} \exp\left(-jk_{xm} u\right)] \quad (9)$$

where $\Psi^{(p)}$ represents either the transverse electric field for the TE polarization or the transverse magnetic field for the TM polarization, and the superscript p=1,2, and 3 denote the incident, the grating, and the transmission regions, respectively. $A_q^{(p)}$s and $B_q^{(p)}$s are the yet unknown coefficients which are to be determined once the boundary conditions are duly applied. m, $q \in [-N, N]$, N stands for the truncation order of the Fourier series, $\lambda_q^{(p)}$ and $\Psi_{mq}^{(p)}$ are the square root of the qth eigenvalue, and the mth component of the qth eigenvector in the standard eigenvalue problem given in equation (5) for the TE polarization and in equation (6) for the TM polarization, respectively. Furthermore, the $\lambda_q^{(p)}$s are chosen in such a way that

$$\mathrm{Re}\left(\lambda_q^{(p)}\right) + \mathrm{Im}\left(\lambda_q^{(p)}\right) < 0 \quad (10)$$

III. Stable Implementation of The Boundary Conditions

To find the yet unknown coefficients $A_q^{(p)}$ and $B_q^{(p)}$, the transverse electromagnetic fields of the grating region should be matched to those of the incident and transmission regions. This can be accomplished in two different ways.

One simple strategy is that the transverse electromagnetic field within the grating, i.e. $\Psi^{(2)}$, is first transformed back to the original Cartesian coordinate system (x,y,z), and then gets matched to the Rayleigh expansion without the grating region [23]. In the first step, the electromagnetic field distribution, which in its current form is expressed as a Floquet's harmonic expansion in the u space, ought to be written as a Floquet's harmonic expansion in the x space. To this end, the term $\exp(-jk_{xm}u)$ in equation (9) should be projected on the Fourier basis in the x space. This can be easily performed by using the transformation matrix $[\mathbf{T}_{ux}]$ whose (p,m) entry reads as [23]

$$\left[\mathbf{T}_{ux}\right]_{pm} = \frac{1}{\Lambda_G} \int_0^{\Lambda_G} h(u) \exp\left[j\left(k_{xp} x(u) - k_{xm} u\right)\right] du \quad (11)$$

and can be very efficiently calculated by using the fast Fourier transform of $h(u)\exp\left[j\left(k_{xp} x(u) - k_{x0} u\right)\right]$.

By multiplying the transformation matrix $[\mathbf{T}_{ux}]$ with the eigenmatrix including the eigenvectors of the standard eigenvalue problem given in equations (5-6) for the (u,y,z) coordinate system, the eigenmatrix containing the desired set of eigenvectors in the original Cartesian system (x,y,z) can be straightforwardly obtained:

$$\boldsymbol{\Psi}_x^{(2)} = \left[\mathbf{T}_{ux}\right] \boldsymbol{\Psi}^{(2)} \quad (12)$$

where $\boldsymbol{\Psi}^{(2)}$ denotes the eigenmatrix whose (m,q) entry is the mth component of the qth eigenvector in the transformed coordinate system, $\Psi_{mq}^{(p)}$, and the $\boldsymbol{\Psi}_x^{(2)}$ represents the same eigenmatrix in the original Cartesian coordinates. The subscript x shows that the expression is given in the coordinate system (x,y,z).

Once the $\boldsymbol{\Psi}_x^{(2)}$ matrix is calculated, the Floquet's harmonic expansion of the electromagnetic field distribution within the grating region can be obtained without solving the standard eigenvalue problem in the Cartesian coordinate system (x,y,z) given in equations (2-3). This is very important because Toeplitz matrices that appear in the original eigenvalue problem are formed of the slowly-convergent Fourier coefficients of discontinuous profiles with sharp contrasts. It is therefore impossible to extract the eigenvectors directly in the Cartesian coordinates.

In the next step, the electromagnetic field distribution within the grating region is to be matched with the Rayleigh expansion without the grating region. Since the refractive indices of the regions 1 and 3 are homogeneous, the Rayleigh expansion reads as

$$\Psi_x^{(1)} = \exp\left(-j\left(k_{z10} z + k_{x0} x\right)\right) + \sum_{i=-N}^{N} R_i \exp\left(j\left(k_{z1i} z - k_{xi} x\right)\right) \quad (13)$$

in region 1, and

$$\Psi_x^{(3)} = \sum_{i=-N}^{N} T_i \exp\left(-j\left(k_{z3i}\left(z-d\right) + k_{xi} x\right)\right) \quad (14)$$

in region 3. Here, the R_is and T_is denote reflected and transmitted orders, respectively, and

$$k_{zli} = \sqrt{k_0^2 n_l^2 - k_{xi}^2}, \; l = 1,3 \quad (15)$$

Now that all field expressions are available in the original Cartesian coordinates, an unconditionally stable recursive matrix algorithm, e.g. the scattering matrix algorithm, can be applied to find all diffraction efficiencies [24]. In this fashion, solving the eigenvalue problem in the homogeneous regions 1 and 3 is avoided, and the reflection and transmission orders are straightforwardly obtained. This method can be easily extended to analyze multilayer structures, where one should first find the eigenmatrix of every modulated layer in a similar fashion, and then apply the conventional scattering matrix propagation algorithm to extract the diffracted orders. It should be however noticed that, despite all the benefits this strategy offers, the transformation matrix $[\mathbf{T}_{ux}]$ is ill-conditioned and incurs numerical instability if inverted during the calculation. Unfortunately, every unconditionally stable recursive matrix algorithm including the scattering matrix method requires the inversion of the $\boldsymbol{\Psi}_x^{(2)}$ matrix [24], and

therefore of the transformation matrix [$\mathbf{T}_{ux}$]. This approach is then seriously liable to numerical instabilities particularly in the microwave range, where the truncation order is presumably large. This point is clearly demonstrated in section IV, where the condition number of the transformation matrix is plotted versus the truncation order *N*. The observed instabilities are thus due to the ill-conditioned nature of the transformation matrix and have nothing to do with the conventional instabilities of the standard RCWA, which are conventionally associated with the presence of both growing and decaying waves, and which can be avoided by using the seemingly stable recursive matrix algorithms, e.g. scattering matrix.

The other possible strategy is that the continuity condition of the tangential electromagnetic fields at each interface is directly applied at the transformed coordinate system (*u*,*y*,*z*), the reflection and transmission coefficients are found, and the obtained results are then brought back to the original Cartesian coordinate system (*x*,*y*,*z*). Although the eigenvalue problem should be solved in all three regions, the unconditional stability of this method is guaranteed as the ill-conditioned transformation matrix is not to be inversed.

It is however worth noticing that in contrast to the optical case where the former method is unlikely to become unstable and is therefore preferred, the latter approach should be inevitably followed here in the microwave range, where the truncation order is large enough to cause unwanted instabilities. Thus, the second approach is adopted and the S-matrix algorithm is applied directly in the transformed coordinate system (*u*,*y*,*z*), where the layer *s* matrix reads as,

$$\widetilde{S}^{(p)} = \begin{bmatrix} \mathbf{I} & \mathbf{0} \\ \mathbf{0} & \boldsymbol{\varphi}^{(p)} \end{bmatrix} \begin{bmatrix} \boldsymbol{\Psi}^{(p+1)} & -\boldsymbol{\Psi}^{(p)} \\ \mathbf{Q}^{(p+1)} & \mathbf{Q}^{(p)} \end{bmatrix}^{-1} \begin{bmatrix} \boldsymbol{\Psi}^{(p)} & -\boldsymbol{\Psi}^{(p+1)} \\ \mathbf{Q}^{(p)} & \mathbf{Q}^{(p+1)} \end{bmatrix} \cdot \begin{bmatrix} \boldsymbol{\varphi}^{(p)} & \mathbf{0} \\ \mathbf{0} & \mathbf{I} \end{bmatrix} \tag{16}$$

Here, $\mathbf{I}$ is the identity matrix, $\boldsymbol{\varphi}^{(2)}$ is a diagonal matrix whose diagonal elements are $\exp(\lambda_q^{(2)} d)$, $\boldsymbol{\varphi}^{(1)}$ and $\boldsymbol{\varphi}^{(3)}$ are both the identity matrix, the $\boldsymbol{\Psi}^{(p)}$ matrix includes the $\Psi_{mq}^{(p)}$'s, and

$$\mathbf{Q}^{(p)} = \boldsymbol{\Psi}^{(p)} \boldsymbol{\lambda}^{(p)} \tag{17}$$

for TE polarization, and

$$\mathbf{Q}^{(p)} = \left[\left[1/\varepsilon(u)\right]\right] \boldsymbol{\Psi}^{(p)} \boldsymbol{\lambda}^{(p)} \tag{18}$$

for TM polarization. In these expressions, $\boldsymbol{\lambda}^{(p)}$ is a diagonal matrix whose diagonal elements are $\lambda_q^{(p)}$.

At this point, the S-matrix can be recursively obtained in terms of the abovementioned layer *s* matrix [24]. For evaluating the yet unknown $A_q^{(3)}$ and $B_q^{(1)}$; however, only two elements of the S-matrix, viz. S_{11} and S_{21}, are needed

$$S_{11} = \widetilde{s}_{11}^{(2)} \left(\mathbf{I} - \widetilde{s}_{12}^{(1)} \widetilde{s}_{21}^{(2)}\right)^{-1} \widetilde{s}_{11}^{(1)} \tag{19}$$

$$S_{21} = \widetilde{s}_{21}^{(1)} + \widetilde{s}_{22}^{(1)} \widetilde{s}_{21}^{(2)} \left(\mathbf{I} - \widetilde{s}_{12}^{(1)} \widetilde{s}_{21}^{(2)}\right)^{-1} \widetilde{s}_{11}^{(1)} \tag{20}$$

and the transmitted and reflected orders in the transformed coordinate system (*u*,*y*,*z*) can be written as

$$\mathbf{A}^{(3)} = S_{11} \mathbf{A}^{(1)} \tag{21}$$

$$\mathbf{B}^{(1)} = S_{21} \mathbf{A}^{(1)} \tag{22}$$

where $\mathbf{A}^{(1)}$, $\mathbf{A}^{(3)}$, and $\mathbf{B}^{(1)}$ vectors include the incident orders $A_q^{(1)}$, the transmitted orders $A_q^{(3)}$, and the reflected orders $B_q^{(1)}$, respectively.

In contrast to the sought-after $\mathbf{A}^{(3)}$ and $\mathbf{B}^{(1)}$ vectors, $\mathbf{A}^{(1)}$ is the incident wave in the transformed coordinate system (*u*,*y*,*z*) and has only one nonzero element $A_r^{(1)}=1$. The index of the only nonzero element of this vector, *r*, is the same as that of the eigenvalue which is closest to the *z* component of the incident wave-vector, $-jk_{z10} = -jk_0 n_1 \cos\theta$. To fully determine the $\mathbf{A}^{(1)}$ vector, i.e. to extract the index *r*, the eigenvalue $\lambda_r^{(1)} \approx -jk_0 n_1 \cos\theta$ is to be spotted. However, in the particular case when $k_{z1i} = k_{z10}$ for $i \neq 0$, there would be two identical eigenvalues both very close to the tagged value $-jk_0 n_1 \cos\theta$, and consequently the correct index of the nonzero element, *r*, cannot be so easily determined. To overcome this difficulty, the incident angle should be slightly changed to violate the $k_{z1i} = k_{z10}$ condition. The correct index *r* can then be extracted at the slightly changed incident angle. Once the nonzero element of the $\mathbf{A}^{(1)}$ vector, $A_r^{(1)}=1$, is found, the reflection and transmission coefficients in the (*u*,*y*,*z*) coordinate system, i.e. $A_q^{(3)}$ and $B_q^{(1)}$, can be easily determined in terms of the S_{11} and S_{21} elements of the S-matrix.

The reflection and transmission orders in the original Cartesian coordinates, R_i and T_i, can then be calculated by back transformation of the $\mathbf{A}^{(3)}$ and $\mathbf{B}^{(1)}$ vectors. This can be achieved by following a procedure very much like the one used to transform the electromagnetic field distribution within the grating region in the (*u*,*y*,*z*) coordinate system, $\Psi^{(2)}$, back to the original Cartesian coordinate system, $\Psi_x^{(2)}$:

$$\left[T_i\right] = \left[\mathbf{T}_{ux}\right] \boldsymbol{\Psi}^{(3)} \mathbf{A}^{(3)} \tag{23}$$

$$\left[R_i\right] = \left[\mathbf{T}_{ux}\right] \boldsymbol{\Psi}^{(1)} \mathbf{B}^{(1)} \tag{24}$$

The desired diffraction efficiencies can then be calculated by using the Poynting theorem:

$$DE_{1i} = \mathrm{Re}\left(\frac{k_{z1i}}{k_{z10}}\right) \left|R_i\right|^2 \tag{25}$$

for the diffracted orders in region 1, and

$$DE_{3i} = C\, \mathrm{Re}\left(\frac{k_{z3i}}{k_{z10}}\right) \left|T_i\right|^2 \tag{26}$$

for the diffracted orders in region 3. Here, C is a polarization dependent factor which is either 1 for the TE or $(\varepsilon_1/\varepsilon_3)^2$ for the TM polarization.

As already mentioned, the latter strategy of applying the boundary conditions at the transformed coordinate system is unconditionally stable as it does not involve the inverse of the ill-conditioned [$\mathbf{T}_{ux}$] matrix. It should be however noticed that the unconditional stability of this approach is not necessarily held in multilayer structures with different sections each having their own jump points and compositions. In such cases, every modulated layer has its own profile and calls for its own resolution function $h(u)$. It will be therefore impossible to apply all the boundary conditions in one specific coordinate system and one has to invert ill-conditioned transformation matrices to apply the continuity condition of transverse electromagnetic field distribution at each interface. Nevertheless, if a multi-section structure with only a small number of sections is to be considered, then a single coordinate transformation can be found in such a way that a good spatial resolution be simultaneously guaranteed around the discontinuities and jump points of all sections. Naturally, the parametric representation in such a coordinate system has several transition points, i.e. u_l's, corresponding to all the jump points present in every section of the structure. The presence of too many transition points in a multi-section structure with not a small number of sections therefore rein in the convergence rate, and makes the proposed approach somewhat unpractical.

IV. Numerical Examples

As the first numerical example to demonstrate the efficiency and stability of the proposed method, a simple metallic lamellar grating is considered. The grating parameters in accordance with Fig. 1 read as follows: $\varepsilon_1 = \varepsilon_3 = \varepsilon_d = 1$, $\theta = 30°$, $\lambda = \Lambda_G = d = 1$ (cm), and $\sigma = 1.45\times10^5$ (S/cm) for $x_0 < x < x_1 = 0.3\Lambda_G$. In Fig. 2, the overall reflectance of the structure for both major polarizations is plotted versus the truncation order N. First, the proposed unconditionally stable strategy is followed and the obtained numerical results are depicted by solid line. Thanks to the technique of adaptive spatial resolution, a very good convergence rate is observed. Second, the more straightforward approach of applying the boundary conditions in the original Cartesian coordinates [23] is followed, and the unstable numerical results are plotted by dashed line. The incurred instability is further examined in Fig. 3, where the condition number of the transformation matrix is plotted versus the truncation order N. This latter figure clearly validates the arguments presented in the previous section.

As another example, the same metallic lamellar grating is reinvestigated this time in the infrared regime at the free space wavelength of $\lambda = 1.3875$ μm. The metallic region is made of silver whose permittivity is $\varepsilon_m = (0.1 - j8.94)^2$, the incoming TM polarized wave is incident at $\theta = 30°$, and $\Lambda_G = d = \lambda$. The geometrical shape of the grating is the same as before. Inasmuch as the contrast between metallic and dielectric permittivites in the infrared regime is not as high as in the microwave range, the conventional RCWA is still applicable. The results obtained by following each of the two strategies discussed in section III are then compared against those obtained by using the conventional RCWA with the correct Fourier factorization method [17]. This is shown in Fig. 4, where the overall reflectance of the structure is calculated by applying the unconditionally stable ASR technique (solid line), the conventional RCWA with the correct Fourier factorization (dashed line), and the conditionally stable ASR technique (dotted line). This figure shows that the transformation of the coordinate system can considerably improve the convergence rate of the solution. It should be however noticed that applying the boundary conditions at the original Cartesian coordinates incur numerical instability for truncation orders $N > 40$. This numerical instability is attributed to the large condition number of the transformation matrix already plotted in Fig. 3. Fortunately, the numerical convergence is achieved for truncation orders $N > 20$, and in contrast to the first example, the more simple strategy of applying boundary conditions in the original Cartesian coordinate system is working for $20 < N < 40$.

Finally, a compound metallic grating with extremely narrow slits is investigated. This structure is schematically shown in Fig. 5, and is composed of three stacks of aluminum ($\sigma = 1.45\times10^5$ S/cm) each separated by narrow air slits ($\varepsilon_{air} = 1$). The geometrical parameters in accordance with Fig. 5 then read as: $\Lambda_G = 10$ mm, $d = 19.8$ mm, $b = 2a = 0.5$ mm, and $c = 3$ mm. It is assumed that the structure is illuminated by a normally incident TM polarized wave. The zeroth-order transmitted diffraction efficiency, DE_{30}, is then plotted versus frequency in Fig. 6. The obtained results calculated by keeping ($2N+1 = 201$) Fourier terms (solid line) show a very good agreement with the experimental data as reported in [15] (circles). Despite the facts that there are six jump points within each unit cell, that the air slits are quite narrow, and that the structure supports TM polarized resonant anomalies, the proposed Fourier based technique is much faster than the brute force fully numerical techniques, e.g. the FEM or the FDTD. It can provide accurate and stable results very much suitable for studying the role of different grating parameters in controlling diffraction properties of such challenging structures. For instance, the effect of c, i.e. width of the aluminum regions, on shifting the absorption spectrum of the same structure is demonstrated in Fig. 7, where the total absorption of the structure with c=1, 2, and 3 mm is plotted versus frequency. This figure clearly demonstrates that the frequency of the maximum absorption can be controlled by changing c.

V. Conclusion

Numerical analysis of the metallic lamellar gratings at microwave frequencies has been thus far believed to be out of reach of the Fourier modal methods. Thanks to the adaptive spatial resolution technique already proposed in the optical regime, the fast and efficient Fourier based technique is now accessible even at microwave frequencies, where the

permittivity profile of the structure is ultrahigh-contrast and cannot be accurately approximated by using truncated Fourier series. In contrast to the optical regime; however, the appropriate boundary conditions cannot be straightforwardly applied here at microwave frequencies. It is therefore necessary to follow the proposed matrix-based algorithm, which does not need the inversion of the ill-conditioned transformation matrix. This work opens new hopes for fast and efficient modeling of enhanced microwave transmission through metallic gratings with narrow slits.

REFERENCES

[1] S. T. Peng and C. M. Shiao, "Scattering of plane waves by metallic gratings," *IEEE MTT-S Digest,* pp. 879-882, 1994.

[2] R. C. Hall, R. Mittra, K. M. Mitzner, "Scattering from finite thickness resistive strip," *IEEE Trans. Antennas Propag.*, vol. 36, no. 4 pp. 504-510, Apr. 1988.

[3] R. C. Hall, R. Mittra, "Scattering from a periodic array of resistive strips," *IEEE Trans. Antennas Propag.*, vol. 33, no. 9 pp. 1009-1011, Sep. 1985.

[4] D. Fan, "A new approach to diffraction problem of conductor grids, part I parallel-polarized incident plane waves," *IEEE Trans. Antennas Propag.*, vol. 37, no. 1 pp. 84-88, Jan. 1989.

[5] D. Fan, "A new approach to diffraction problem of conductor grids, part I prependicular-polarized incident plane waves," *IEEE Trans. Antennas Propag.*, vol. 37, no. 1 pp. 89-93, Jan. 1989.

[6] K. Uchida, T. Noda and T. Matsunaga, "Electromagnetic wave scattering by an infinite plane metallic grating in case of oblique incidence and arbitrary polarization," *IEEE Trans. Antennas Propag.*, vol. 36, no. 3 pp. 415-422, Mar. 1988.

[7] K. Uchida, T. Noda and T. Matsunaga, "Spectral domain analysis of electromagnetic wave scattering by an infinite plane metallic grating," *IEEE Trans. Antennas Propag.*, vol. 35, no. 1 pp. 46-52, Jan. 1987.

[8] G. Granet and B. Guizal, "Analysis of strip gratings using a parametric modal method by Fourier expansions," *Opt. Commun.*, vol. 255, no. 1, pp. 1-11, 2005.

[9] T. W. Ebbesen, H. J. Lezec, H. F. Ghaemi, T. Thio and P. A. Wolff, "Extraordinary optical transmission through sub-wavelength hole arrays," *Nature*, vol. 391, no. 6668, pp. 667-669, Feb. 1998.

[10] A. P. Hibbins, J. R. Sambles and C. R. Lawrence, "Grating-coupled surface plasmons at microwave frequencies," *J. Appl. Phys.*, vol. 86, no. 4, pp. 1791-1795, Aug. 1999.

[11] A. P. Hibbins, J. R. Sambles and R. C. Lawrence, "The coupling of microwave radiation to surface plasmon polaritons and guided modes via dielectric gratings," *J. Appl. Phys.*, vol. 87, no. 6, pp. 2677–2683, Mar. 2000

[12] S. S. Akarca-Biyikli, I. Bulu and E. Ozbay, "Enhanced transmission of microwave radiation in one-dimensional metallic gratings with subwavelength aperture," *Appl. Phys. lett.*, vol. 85, no. 7, pp. 1098-1100, Aug. 2004.

[13] H. Caglayan, I. Bulu and E. Ozbay, "Extraordinary grating-coupled microwave transmission through a sub wavelength annular aperture," *Opt. Express*, vol. 13, no. 5, pp. 1666-1671, Mar. 2005.

[14] Y. G. Ma, X. S. Rao, G. F. Zhang and C. K. Ong, "Microwave transmission modes in compound metallic gratings," *Phys. Rev. B,* vol. 76, no. 8, pp. 085413(5), Aug. 2007.

[15] A. P. Hibbins, I. R. Hooper, M. J. Lockyear and J. R. Sambles, "Microwave transmission of a compound metal grating," *Phys. Rev. Lett.*, vol. 96, no. 25, pp. 257402(4), June 2006.

[16] S. S. Akarca-Biyikli, I. Bulu and E. Ozbay, "Resonant excitation of surface plasmons in one-dimensional metallic grating structures at microwave frequencies," *J. Opt. A.: Pure Appl. Opt.*, vol. 7, no. 2, pp. 159-164, Jan. 2005.

[17] L. Li, "use of Fourier series in the analysis of discontinuous periodic structures," J. Opt. Soc. Am. A, vol. 13, no. 9, pp. 1870-1876, Sep. 1996.

[18] M. Nevière and E. Popov, *Light Propagation in Periodic Media: Differential Theory and Design.* Marcel Dekker, NewYork, 2003

[19] A. Khavasi, K. Mehrany and B. Rashidian, "Three-dimensional Diffraction Analysis of gratings Based on Legendre Expansion of Electromagnetic Fields, " *J. Opt. Soc. Am. B*, vol. 24**,** no. 10, pp. 2676-2685, Oct. 2007.

[20] C. Kittel, "Introduction to solid state physics," John Wiley & Sons, New York, 1996.

[21] G. Granet, "Reformulation of lamellar grating problem through the concept of adaptive spatial resolution," *J. Opt. Soc. Am. A*, vol. 16**,** no. 10, pp. 2510-2516, Oct. 1999.

[22] G. Granet, J. Chandezon, J. P. Plumey, and K. Raniriharinosy, ''Reformulation of the coordinate transformation method through the concept of adaptive spatial resolution. Application to trapezoidal gratings,'' *J. Opt. Soc. Am. A*, vol. 18, no. 9, pp. 2102–2108, Sep. 2001.

[23] T. Vallius and M. Honkanen "Reformulation of the Fourier modal method with adaptive spatial resolution: application to multilevel profiles," *Opt. Express*, vol. 10, no. 1, pp. 24-34, Jan. 2002.

[24] L. Li, "Formulation and comparison of two recursive matrix algorithms for modeling layered diffraction gratings," *J. Opt. Soc. Am. A.*, vol. 13, no. 5, pp. 1024-1035, May 1996.

Amin Khavasi was born in Zanjan, Iran, on January 22, 1984. He received the B.Sc. and M.Sc degrees both in electrical engineering from Sharif University of Technology, Tehran, Iran in 2006, and 2008, respectively. He is currently working toward the Ph.D. degree at Sharif University of Technology.

His research interests include photonics and computational electromagnetic.

Khashayar Mehrany was born in Tehran, Iran, on September 16, 1977. He received the B.Sc., M.Sc., and Ph.D. (*magna cum laude*) degrees from Sharif University of Technology, Tehran, Iran, in 1999, 2001, and 2005, respectively, all in electrical engineering.

Since then, he has been an Assistant Professor with the Department of Electrical Engineering, Sharif University of Technology. His research interests include photonics, semiconductor physics, nanoelectronics, and numerical treatment of electromagnetic problems.

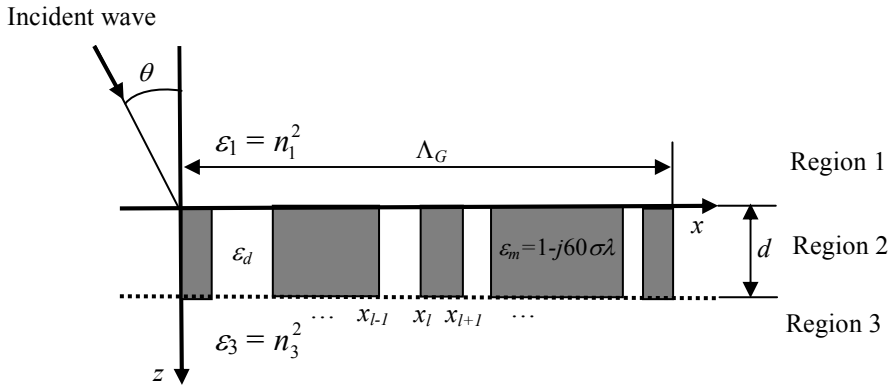

Fig. 1. A typical metallic lamellar grating.

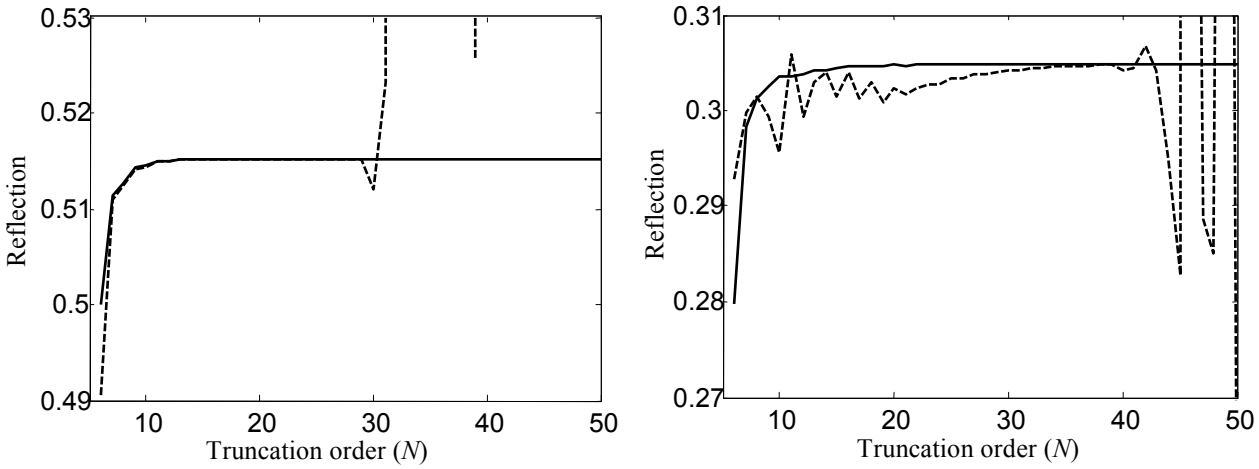

(a) (b)

Fig. 2. The electromagnetic reflectance of a simple metallic lamellar grating versus the truncation order N calculated by using the proposed method (solid line) and the optical approach of applying the boundary conditions at the original Cartesian coordinates: (a) for TE polarization and (b) for TM polarization.

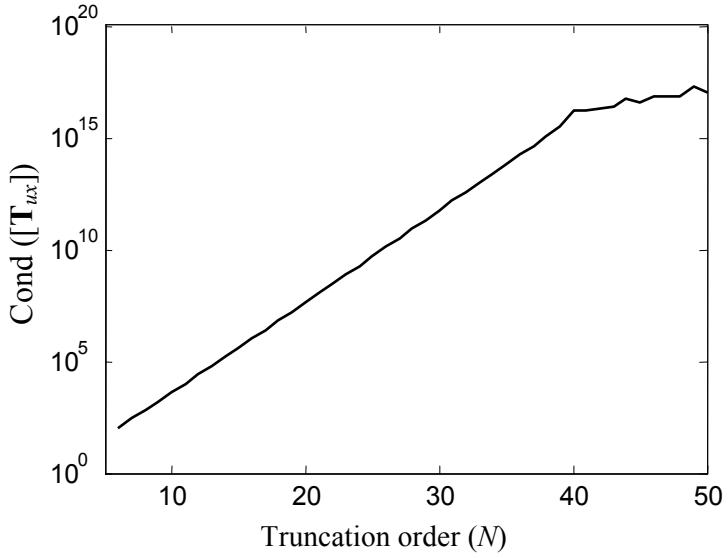

Fig. 3. Condition number of the transformation matrix, [$\mathbf{T}_{ux}$], versus the truncation order N.

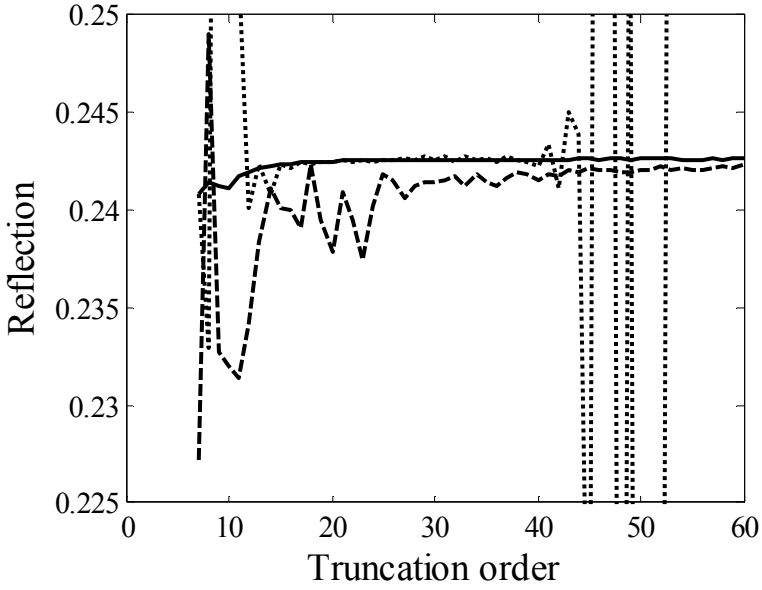

Fig 4. Reflection of a simple metallic lamellar grating versus truncation order in the infrared regime calculated by using the conventional RCWA (dashed line), the proposed adaptive spatial resolution technique (solid line), and the optical approach of applying the boundary conditions at the original Cartesian coordinates (dotted line).

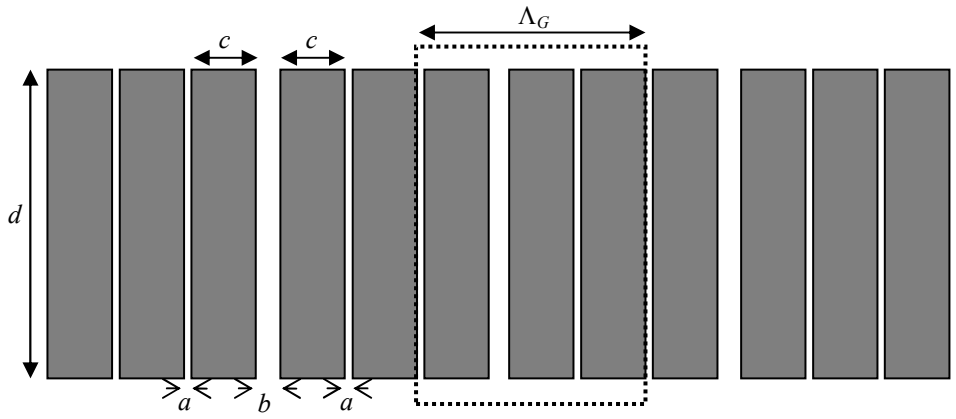

Fig. 5. A compound metallic grating with three narrow slits in each unit cell.

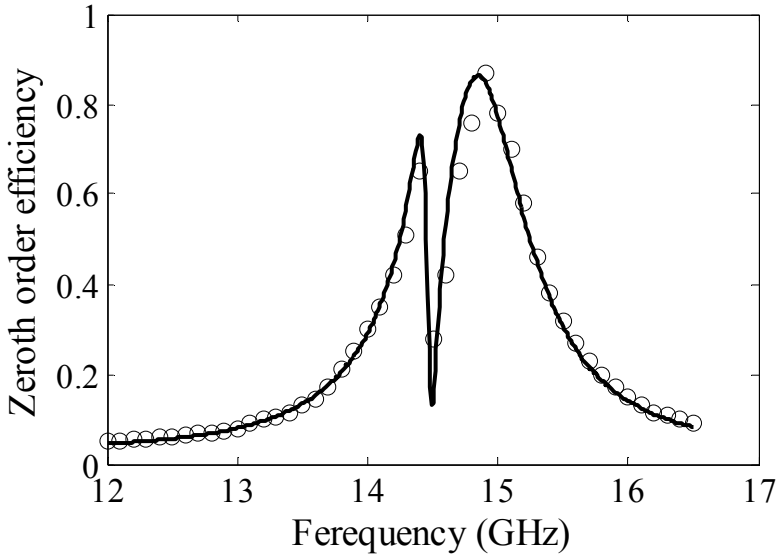

Fig. 6. The zeroth-order transmitted diffraction efficiency of the compound metallic grating illustrated in Fig.4: Λ_G = 10 mm, d = 19.8 mm, $b = 2a$ = 0.5 mm and c = 3 mm, calculated by propose method (solid line). The experimental results as reported in [15] are also presented by circles.

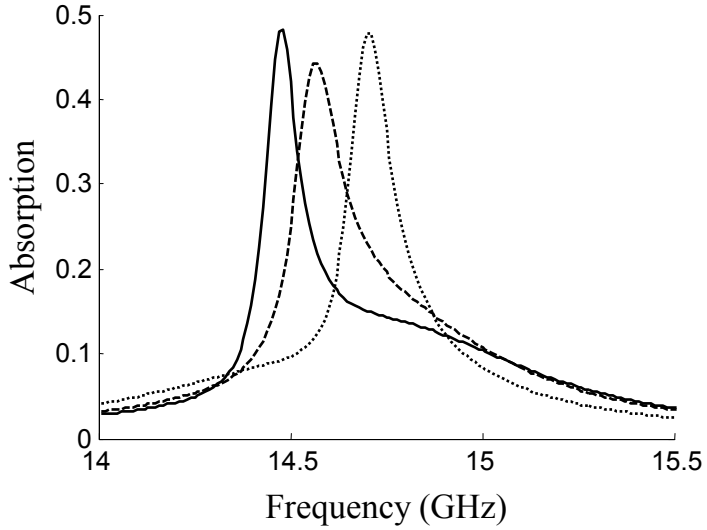

Fig. 7. The absorption spectrum of the same compound grating with *c*=1 mm (dotted line), 2(dashed line) and 3 mm (solid line).